NOISE SUPPRESSION DUE TO
ANNULUS SHAPING OF A
CONVENTIONAL COAXIAL NOZZLE

U. von Glahn and J. Goodykoontz
Lewis Research Center
Cleveland, Ohio

NOISE SUPPRESSION DUE TO ANNULUS SHAPING OF A

CONVENTIONAL COAXIAL NOZZLE

by U. von Glahn and J. Goodykoontz

National Aeronautics and Space Administration
Lewis Research Center
Cleveland, Ohio 44135

ABSTRACT

Previous studies have shown that increasing the annulus width of a conventional coaxial nozzle with constant bypass velocity will lower the noise level. In the present model-scale study, the annulus was shaped by an eccentric mounting of the annular nozzle with respect to the conical core nozzle. Acoustic measurements were made in the flyover plane below the widest portion of the annulus and at 90° and 180° from this point. The model-scale spectra are scaled up to engine size (1.07 m diameter) and the perceived noise levels for the eccentric and concentric coaxial nozzles are compared over a limited range of operating conditions. The implications of the acoustic benefits derived from the eccentric nozzle to practical applications are discussed.

INTRODUCTION

Experimental data obtained with coaxial bypass nozzles (ref. 1) indicate that jet noise suppression increases with increasing radius ratio of the outer low velocity stream. From this consideration, a two-stream bypass nozzle concept was evolved in which nozzle shaping through an asymmetrical exhaust nozzle flow passage conceivably could provide additional acoustic benefits over that of a concentric baseline bypass nozzle. (The latter bypass nozzle would already be more quiet than a reference conical nozzle.) In the present study, simple nozzle shaping for noise reduction was obtained by modifying an existing concentric coaxial nozzle used in previous acoustic studies (refs. 2 and 3). The nozzle was modified such as to provide an eccentric outer stream annulus, while maintaining approximately the same through-flow as that, for the original concentric bypass nozzle. This alteration provided a wide annulus at one point of the outer nozzle and a narrow annulus at 180° or opposite this widest point, with a varying annulus width between these two points (fig. 1). The outer stream jet velocity was constant around the circumference of the eccentric annulus at the exhaust plane. It should be noted that with an inverted-velocity-profile nozzle, suppression is obtained with the narrow portion of the annulus in the flyover plane (ref. 4) in contrast to the present configuration in which suppression is obtained with the wide portion of the annulus in the flyover plane.

As a consequence of the varying circumferential velocity decay around the annulus, skewed velocity profile should exist in the downstream portion of the exhaust plume, with maximum and minimum velocities in the outer stream corresponding to the widest and narrowest portions of the eccentric annulus. Peak jet noise reductions would be expected to result in a direction below the maximum outer stream annulus width, which is an aircraft application would be the flyover plane. In a prac-tical case, sideline noise reductions are of equal or greater importance compared with the flyover values. The present nozzle concept has less noise reduction as the circumferential angle increases from the flyover position because the outer stream annulus width decreases with increas-ing circumferential angle. Practical applications in which the annu-lus height would be shaped and be maintained at a constant wide width for 80° to 120° from the flyover plane are discussed in the paper.

This paper then presents the results of an exploratory experimental program to determine the noise generating characteristics of an eccen-tric coaxial bypass nozzle over a range of flow conditions. The results are compared with those for a concentric coaxial nozzle (refs. 2 and 3). Nominal temperatures ranged from 280 to 1100 K, with nozzle pressure ra-tios ranging from 1.4 to 2.2, for the inner stream and a constant 1.4 for the outer stream.

APPARATUS AND PROCEDURE

Facility

A photograph of the flow facility is shown in figure 2. A common source of unheated laboratory air was used to supply flow for two paral-lel flow lines; one line for the inner nozzle and the other for the outer nozzle. Each flow line had its own air and fuel flow control and flow measuring systems. The air in each line was heated by jet engine com-bustors. Mufflers in each line attenuated flow control valve noise and internal combustion noise. The system was designed to give maximum noz-zle exhaust temperatures of 1100 K and nozzle pressure ratios up to 3.0 in both the inner and outer stream flow lines.

Acoustic. - A sideline microphone array was used for the tests de-scribed herein. Microphones were placed at a constant 5.0 meters dis-tance from and parallel to the nozzle axis, as shown in figure 3. The centerline microphone array consisted of 0.635 cm condenser microphones with the metal protective grids removed to improve the acoustic perform-ance at high frequencies. The locations of the microphones were selec-ted to accommodate other acoustic test programs (ref. 2). The ground-plane of the test area was composed of asphalt interspersed with patches of concrete and covered with 15.25 cm thick foam rubber blankets.

Nozzles

Two coaxial nozzle configurations were used in the experimental program; one with a concentric, coplanar exit, and one with an eccentric coplanar exit. Pertinent dimensions of the nozzles are given in figure 4. The area ratio of the nozzle was 1.4 and is defined as the ratio of the outer nozzle flow area to the inner nozzle flow area. The diameters shown in the figure are inside diameters of the respective nozzles. Photographs of the concentric and eccentric coplanar nozzles are shown in figure 5. The outer wall of the inner nozzle was coated with a high temperature ceramic material to minimize heat transfer between the two streams during coplanar operation. The interior of the upstream portion of the inner nozzle supply line was also lined with insulating material.

Procedure

Steady-state conditions were attained for each test before the data were recorded. Upstream total temperatures and total pressures for both streams were then automatically recorded, as were the acoustic data.

In the acoustic tests, the noise signals from the microphone were sequentially analyzed on-line, and 1/3-octave-band sound pressure levels were digitally recorded on magnetic tape for further processing. Acoustic measurements were made in a plane passing through the minimum and maximum annulus width points, as well as at 90° to this plane by rotating the outer nozzle about its axis.

In order to obtain full-scale perceived noise levels, PNL, the model-scale noise spectra were scaled for size (equivalent nozzle diameter of 1.07 m), distance, and atmospheric attenuation and frequency-shifted using the Strouhal relationship. From such full-scale spectra PNL values were computed for a standard day (288 K at 70% R.H.) at a flyover height of 338 m.

From plots of full-scale PNL values as a function of distance along the flight path, a flyover relative noise level (FRNL) was computed as described in appendix A of reference 5. The term "relative" is used herein since the conventional definition of effective perceived noise level (EPNL) includes forward flight effects, whereas the present data are for static conditions. The omission of flight effects, however, does not significantly affect the present flyover relative noise level comparisons between the various configurations. Comparisons of relative flyover noise levels of the concentric and eccentric nozzles were then made.

Summary of Flow Conditions

The flow conditions used in the present acoustic study are summarized in the following table.

NOMINAL NOZZLE FLOW CONDITIONS

Operational mode	PR_o	T_o, K	V_o, m/s	PR_i	T_i, K	V_i, m/s	V_o/V_i
All subsonic	1.4	288	232	1.8	1089	601	0.39
	1.4	288	229	1.4	533	338	.68
Supersonic V_i, Subsonic V_o	1.4	288	229	2.2	533	495	.46

MODEL-SCALE SPECTRAL DATA

Representative measured spectral data in the flyover plane ($\varphi = 0°$) for the concentric nozzle obtained at model scale are compared with those for the eccentric nozzle in figure 6. The data shown are for a radiation angle, ϑ, of 129° and the flow conditions given in the figure. It is apparent that for this radiation angle, a significant suppression in SPL is obtained with the eccentric nozzle for model scale frequencies greater than about 1000 hertz. For frequencies below 1000 hertz, the spectra for the two nozzles indicate that little noise suppression is obtained with the eccentric nozzle. Also shown on the abscissa in the figure is a second scale that identifies the frequencies and sound pressure level region associated with a full-size engine having an equivalent nozzle diameter of 1.07 m (total exhaust area of 0.9 m^2). Hereinafter, all the acoustic data will be scaled to and presented for this engine size.

ENGINE-SIZE SPECTRA

In the following section, representative spectra for several conceptual engine cycles are presented for both the eccentric and concentric nozzles at engine size. The engine cycle concepts consist of: (1) both streams subsonic and (2) inner stream supersonic and outer stream subsonic.

Flyover Plane ($\varphi = 0°$)

For each of the preceding cycle concepts, representative engine-size spectra will be shown for the forward quadrant ($\vartheta = 46°$), nearly overhead flyover ($\vartheta = 95°$), and rear quadrant ($\vartheta = 129°$).

Forward quadrant (θ = 46°). - The spectra for both the eccentric and concentric nozzles are shown in figure 7 for the two engine cycle concepts. In general, with both streams subsonic (fig. 7(a)) no noise suppression is obtained with the eccentric nozzle. (The apparent suppression at frequencies less than 200 hertz is believed due, in large part, to ground reflections.) With a supersonic core stream (fig. 7(b)), however, the spectrum for the eccentric nozzle is suppressed for all frequencies compared to that obtained with the concentric bypass nozzle. As will be shown later, the eccentric nozzle was louder than the concentric nozzle when the subsonic core stream velocity was reduced from 601 to 338 m/s with a constant outer stream nominal velocity of 230 m/s.

Flyover (θ = 95°). - Representative spectra for the two-cycle concepts are shown in figure 8 for a nearly overhead flyover location. In general, the spectra for the eccentric and concentric nozzles are the same. Any apparent deviation of the data appear to be within data repeatability and/or associated with ground reflections in the test arena. Consequently, the eccentric nozzle shows no significant acoustic benefits over the concentric nozzle at the overhead flight position.

Rear quadrant (θ = 129°). - Representative spectra for the illustrative engine cycles are shown in figure 9 near the peak noise angle in the flyover plane. In all cases, the eccentric nozzle provided noise suppression compared with noise produced by the concentric nozzle. In general, the spectral reductions occurred at engine-size frequencies greater than 100 hertz.

Sideline (φ = 90°) and Overhead (φ = 180°)

In general, the SPL for the eccentric nozzle at φ of 90° and 180° (see fig. 1) were significantly higher (locally up to 5 dB) than thos for the concentric nozzle. At high radiation angles (θ = 139° to 148°), the overhead (φ = 180°) SPL values for the narrow portion of the annulus were locally as much as 10 dB greater with the eccentric nozzle compared with those for the concentric nozzle.

Effect of Cycle Conditions on Spectra

The effect of changing the inner stream velocity while maintaining the outer stream velocity constant is shown in figure 10 for radiation angles of 46°, 68°, 95°, 115°, 129°, 139°, and 148°. The data are shown as an SPL difference between the concentric and eccentric nozzle, ΔSPL = SPL_E - SPL_C, as a function of engine-size frequency. In general, the greatest suppression in the forward quadrant was obtained with the supersonic core stream velocity. An apparent increase in SPL was obtained with the lowest core stream velocity (338 m/s). In the rear quadrant, the least

SPL suppression was obtained with the lowest core stream velocity. In the region of $\theta = 129^\circ$ and 139°, the greatest SPL suppression was obtained with a high subsonic core stream. However, at $\theta = 148^\circ$, the supersonic core stream spectrum indicated the greatest SPL suppression. Because of the limited data, general trends in the local SPL values with operating conditions however, cannot be ascertained with any degree of confidence.

PERCEIVED NOISE LEVELS

From the measured spectra for the concentric and eccentric nozzles, the engine-size perceived noise levels (PNL) were calculated as a function of distance along the flight path. A representative variation of PNL as a function of distance along the flight path is shown in figure 11. For the specific operating conditions noted on the figure, it is apparent that significant noise reduction is obtained with the eccentric nozzle in the PNL region important for noise certification (i.e., 10 PNdB down from the peak PNL value).

The reduction in PNL obtained by use of the eccentric nozzle is shown in figure 12 for all flow conditions in terms of a $\Delta PNL = PNL_E - PNL_C$ as a function of the distance along the flight path. The data show that the PNL values for the eccentric nozzles are suppressed significantly in the rear quadrant and to a lesser extent in the forward quadrant. Maximum suppressions of about 3 to 6 PNdB were obtained at the peak noise angles for the cycle concepts included in the study. The most effective PNL suppressions in the forward quadrant were obtained with a supersonic inner stream (fig. 12(b)).

In general, as indicated in the discussion of SPL trends, the noise level of the eccentric nozzle was significantly higher at $\varphi = 90^\circ$ and 180° than that of the concentric nozzle. The PNL differences between the eccentric and concentric nozzles for $\varphi = 180^\circ$ are shown in figure 13 as a function of distance along the flight path. Similar results were obtained at $\varphi = 90^\circ$.

FLYOVER RELATIVE NOISE LEVEL

From PNL plots, such as that shown in figure 11, flyover relative noise levels (FRNL) were calculated by the method of reference 5. The change in FRNL values between the concentric and eccentric nozzles for the three flow operating conditions included herein are shown in the following table as $\Delta FRNL = FRNL_E - FRNL_C$.

SUMMARY OF FLYOVER RELATIVE NOISE LEVELS

Operational mode	V_o, m/s	V_i, m/s	PR_o	PR_i	V_o/V_i	$\Delta FRNL$, EPNdB
All subsonic	232	601	1.4	1.8	0.39	-3.2
	229	338	1.4	1.4	.68	-1.4
Supersonic V_i, Subsonic V_o	229	495	1.4	2.2	.46	-3.2

As shown in the preceding table, $\Delta FRNL$ values of -1.4 to -3.2 EPNdB are achieved with the eccentric nozzle when compared with the concentric nozzle noise levels. Also shown is that higher $\Delta FRNL$ values are obtained with V_o/V_i ratios near 0.4 than with that near 0.7.

PRACTICAL APPLICATION CONSIDERATIONS

For purposes of practical application noise suppression is generally desired both in the sideline plane ($\varphi = 65°$) and the flyover plane ($\varphi = 0°$). The eccentric nozzle provides maximum suppression in the flyover plane, with decreasing suppression as φ increases toward $90°$. However, by shaping the annulus with a constant wide width to $\varphi = 90°$, or even greater, sideline suppression should be achievable. By following this procedure, the annulus width must be decreased for φ values larger than the φ_{max} for the wide width annulus. This, in essence, yields an asymmetric annulus (fig. 14) for the present nozzle concept.

Consider now nozzle shaping as a concept for plug-type nozzles. Data, not included herein, obtained with the present eccentric nozzle with flow in the annulus only (inner stream flow shutoff), showed noise reductions occurring in the rear quadrant. This is perhaps indicative of what might occur with a single stream plug nozzle. The magnitude of the reductions were similar to those obtained with both streams flowing. The noise reduction was obtained with the narrow portion of the annulus oriented in the flyover plane.

In figure 15 is shown a possible two-stream plug nozzle concept utilizing nozzle shaping to obtain additional noise suppression over the respective baseline configuration based on the previous discussion and data included herein. The nozzle configuration shown consists of a conventional bypass nozzle concept utilizing an inner stream plug nozzle and an outer stream annular nozzle. For this case, inner annulus has the narrow portion of the annulus in the flyover and sideline planes whereas the outer annulus has the wide portion of the annulus in these planes.

It is expected that further substantial noise suppression can be achieved with shaped nozzles by incorporating suppressor elements into the design concept. Such nozzle concepts could consider both full core stream suppressors, or partial core stream suppressors. The application of such suppressors could not only reduce the jet noise but could enhance the usual suppressor noise reduction of the baseline nozzles by advantageously altering the jet plume velocity profile.

CONCLUDING REMARKS

From a brief experimental exploratory study, it has been determined that additional directional noise suppression benefits can be obtained with nozzle shaping compared with those obtained with a baseline nozzle. The noise benefits were obtained with an eccentric coaxial nozzle applicable to subsonic aircraft. Applications of the study to other bypass nozzle concepts indicated potential benefits for coannular plug-type nozzles. Effects of non-coplanar two-stream nozzle arrangements on the potential benefits of nozzle shaping remain to be assessed.

APPENDIX A

SYMBOLS

EPNL   effective perceived noise level, EPNdB

FRNL   flyover relative noise level, EPNdB

PNL   perceived noise level, PNdB

PR   stream pressure ratio

SPL 1/3-octave-band sound pressure level, dB re 20μ N/m^2

T   stream total temperature

V   stream velocity

φ circumferential angle (fig. 1)

θ radiation angle

Subscripts:

C   concentric

E   eccentric

i   inner stream

o   outer stream

REFERENCES

1. W. Olsen and R. Friedman, "Jet Noise from Co-Axial Nozzles Over a Wide Range of Geometric and Flow Parameters," NASA TM X-71503 (1974).

2. J. H. Goodykoontz and J. R. Stone, "Experimental Study of Coaxial Nozzle Noise," AIAA Paper No. 79-631 (Mar. 1979), also NASA TM-79090 (1979).

3. J. R. Stone, J. H. Goodykoontz, and O. A. Gutierrez, "Effects of Geometric and Flow-Field Variables on Inverted-Velocity-Profile Coaxial Jet Noise," AIAA Paper No. 79-635 (Mar. 1979), also NASA TM-79095 (1979).

4. J. Goodykoontz and U. von Glahn, "Noise Suppression Due to Annulus Shaping of an Inverted-Velocity-Profile Coaxial Nozzle," To be presented at the 99th Meeting of the Acoustical Society of America, Atlanta, GA (Apr. 21-25, 1980), also NASA TM-81460 (1980).

5. D. Groesbeck and U. von Glahn, "Assessment at Full Scale of Nozzle/Wing Geometry Effects on OTW Aeroacoustic Characteristics," NASA TM-79168 (1979).
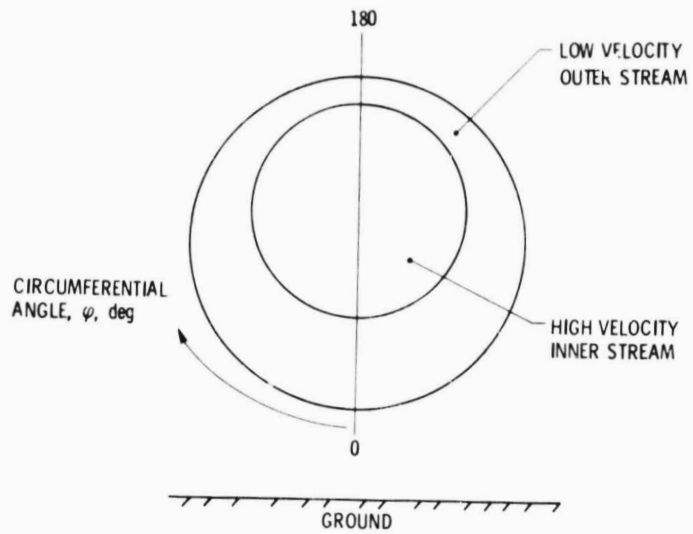
Figure 1. - Eccentric conventional-bypass nozzle.
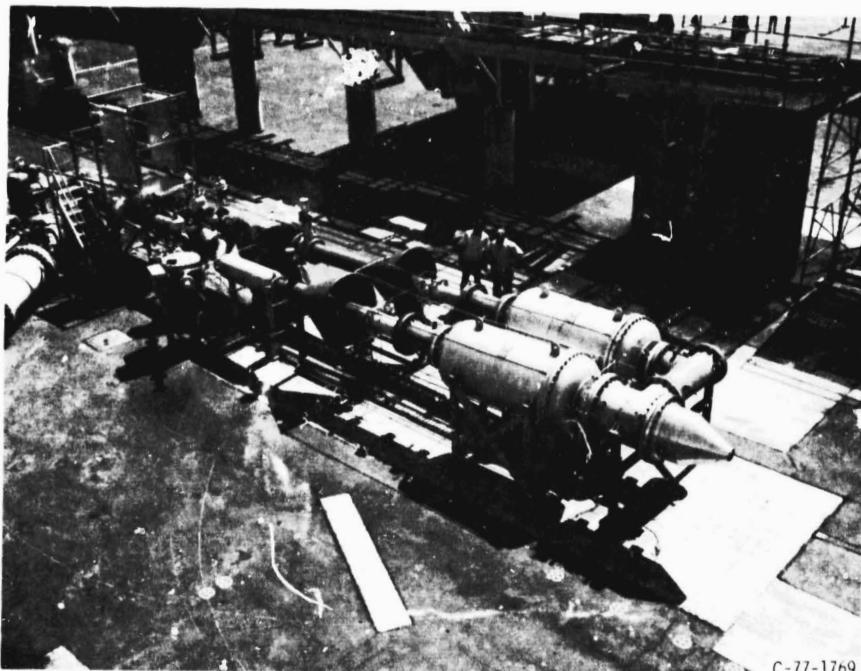
Figure 2. - Coaxial jet flow facility.

NOZZLE AXIS A

θ

CENTERLINE MICROPHONE
LOCATIONS

θ 46° 68° 95° 115° 129° 139° 148° 151°

A

(a) PLAN VIEW.

0.635 cm CENTERLINE MICROPHONE

NOZZLE CENTERLINE

1.7 m

15.25 cm FOAM RUBBER

5.0 m

GRADE (ASPHALT)
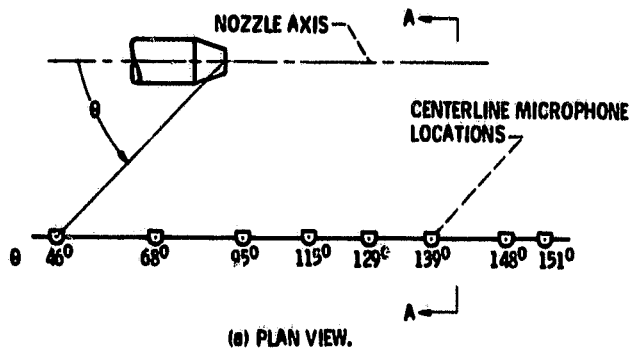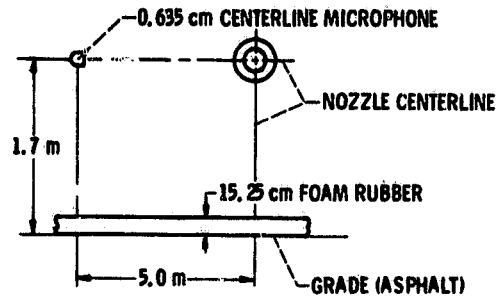
(b) ELEVATION VIEW, VIEW A-A.

Figure 3. - Microphone layout.

42.8 cm   57.5 cm

49.7 cm

76.2 cm DIAM

27.6°

38.3 cm DIAM
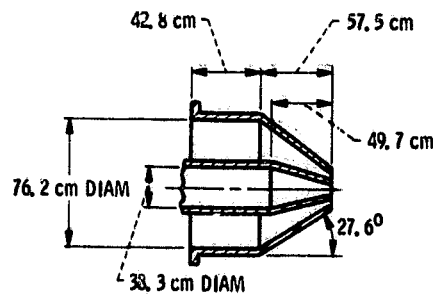
(a) BASIC NOZZLE DIMENSIONS.

0.38

10.1   16
DIAM DIAM

1.8
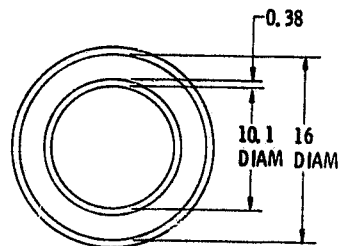
(b) EXIT CROSS-SECTION, CONCENTRIC
NOZZLE.
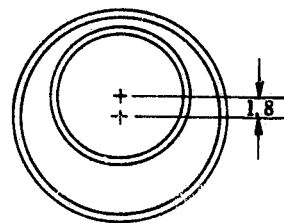
(c) EXIT CROSS SECTION, ECCENTRIC
NOZZLE.

Figure 4. - Schematic of coaxial nozzles. All dimensions in centimeters.
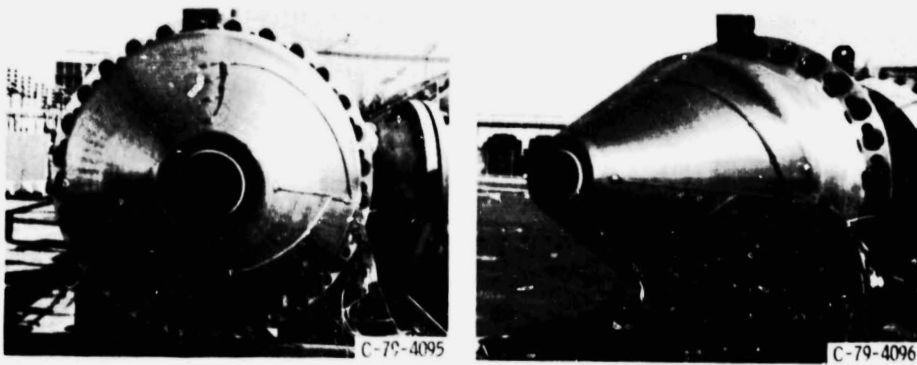
(a) CONCENTRIC NOZZLE.
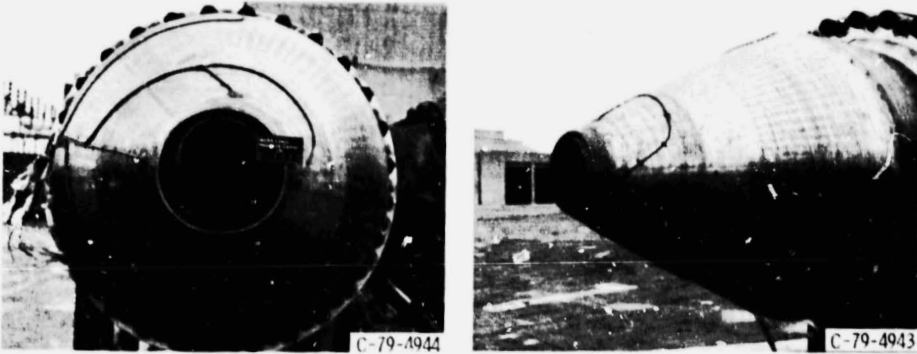

(b) ECCENTRIC NOZZLE.

Figure 5. - Photographs of concentric and eccentric nozzles.
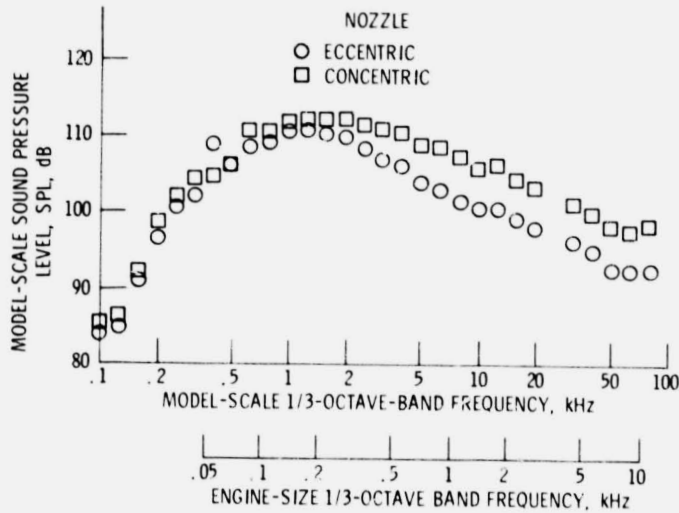


Figure 6. - Illustration of model-scale spectra applicable to engine size noise characteristics. Radiation angle, θ, 129°; PR_i, 2.2; PR_0, 1.4; V_0, 496 m/s; V_i, 229 m/s; engine/model nozzle scale factor, 6.9; φ, 0°.

NOZZLE
O ECCENTRIC
□ CONCENTRIC

NOMINAL:
PR_o = 1.4
PR_i = 1.8
V_o, m/s = 232
V_i, m/s = 601

(a) BOTH STREAMS SUBSONIC.

NOMINAL:
PR_o = 1.4
PR_i = 2.2
V_o, m/s = 229
V_i, m/s = 495

ENGINE-SIZE SOUND PRESSURE LEVEL, SPL, dB

(b) INNER STREAM SUPERSONIC, OUTER STREAM SUBSONIC.
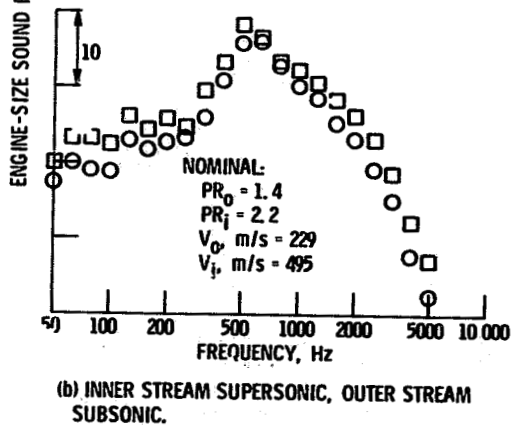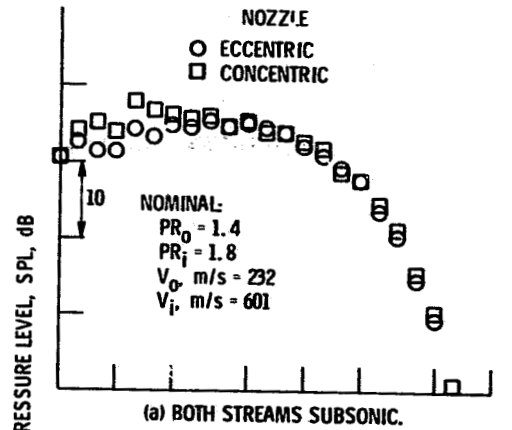
Figure 7. – Representative spectra at 46° radiation angle. φ, 0°.

NOZZLE
O ECCENTRIC
□ CONCENTRIC

NOMINAL:
PR_o = 1.4
PR_i = 1.8
V_o, m/s = 232
V_i, m/s = 601

(a) BOTH STREAMS SUBSONIC.

NOMINAL:
PR_o = 1.4
PR_i = 2.2
V_o, m/s = 229
V_i, m/s = 495

ENGINE-SIZE SOUND PRESSURE LEVEL, SPL, dB

FREQUENCY, Hz

(b) INNER STREAM SUPERSONIC, OUTER STREAM SUBSONIC.
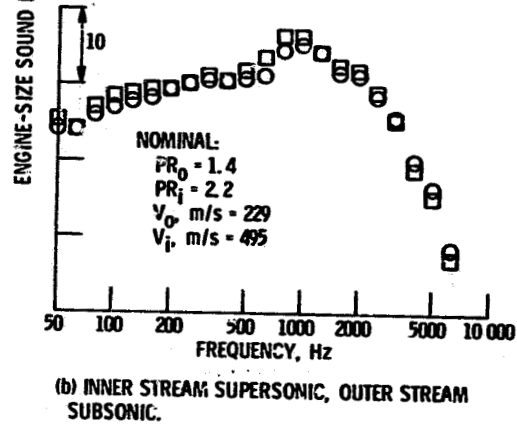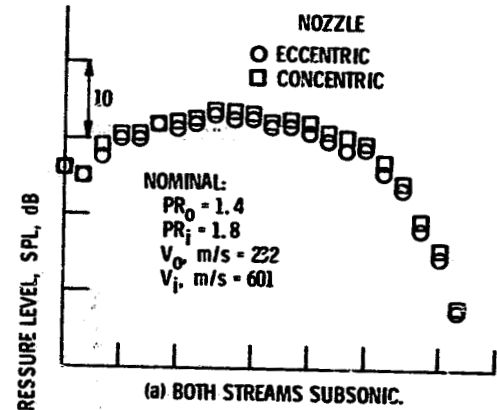
Figure 8. – Representative spectra at 95° radiation angle. φ, 0°.
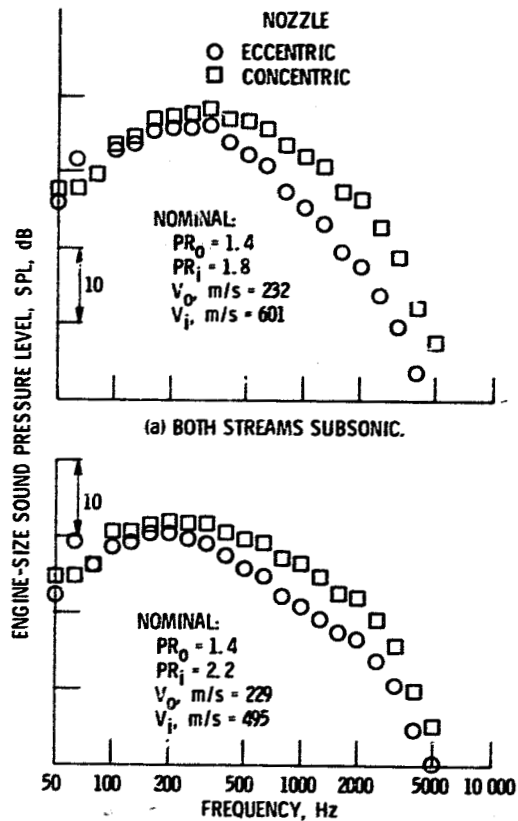
Figure 9. - Representative spectra at 129° radiation angle. φ, 0°.

(a) BOTH STREAMS SUBSONIC.

(b) INNER STREAM SUPERSONIC, OUTER STREAM SUBSONIC.

NOZZLE
○ ECCENTRIC
□ CONCENTRIC

NOMINAL:
PR_0 = 1.4
PR_i = 1.8
V_0, m/s = 232
V_i, m/s = 601

NOMINAL:
PR_0 = 1.4
PR_i = 2.2
V_0, m/s = 229
V_i, m/s = 495

ENGINE-SIZE SOUND PRESSURE LEVEL, SPL, dB

FREQUENCY, Hz

V_0, m/s	V_i, m/s	PR_0	PR_i
232	601	1.4	1.8
229	338	1.4	1.4
229	495	1.4	2.2

(a) RADIATION ANGLE, θ, 46°.

(b) RADIATION ANGLE, θ, 68°.

(c) RADIATION ANGLE, θ, 95°.

(d) RADIATION ANGLE, θ, 115°.

CHANGE IN ENGINE-SIZE SOUND PRESSURE LEVEL, SPL_E - SPL_C, dB

FREQUENCY, Hz

Figure 10. - Variation of SPL_E - SPL_C with flow conditions.

(e) RADIATION ANGLE, θ, 129⁰.

(f) RADIATION ANGLE, θ, 139⁰.

Figure 10. - Continued.

(g) RADIATION ANGLE, θ, 148⁰.

Figure 10. - Concluded.

NOZZLE
○ ECCENTRIC
□ CONCENTRIC

RADIATION ANGLE, θ, deg

46   68   95   115   129   139   148

PERCEIVED NOISE LEVEL, PNL, PNdB

400   200   0   -200   -400   -600
DISTANCE ALONG FLIGHT PATH, m
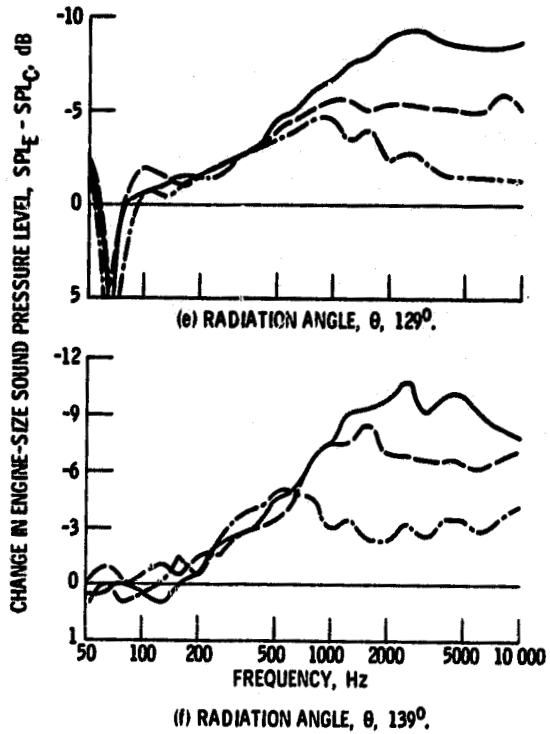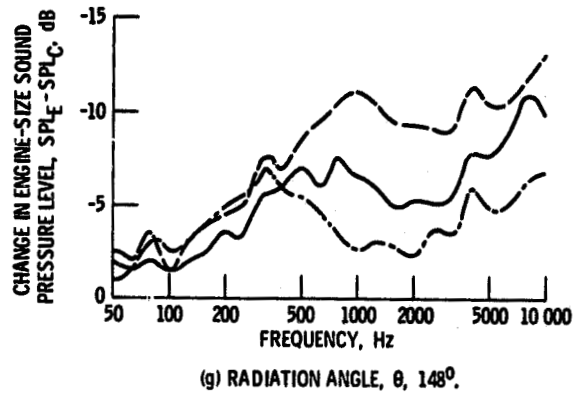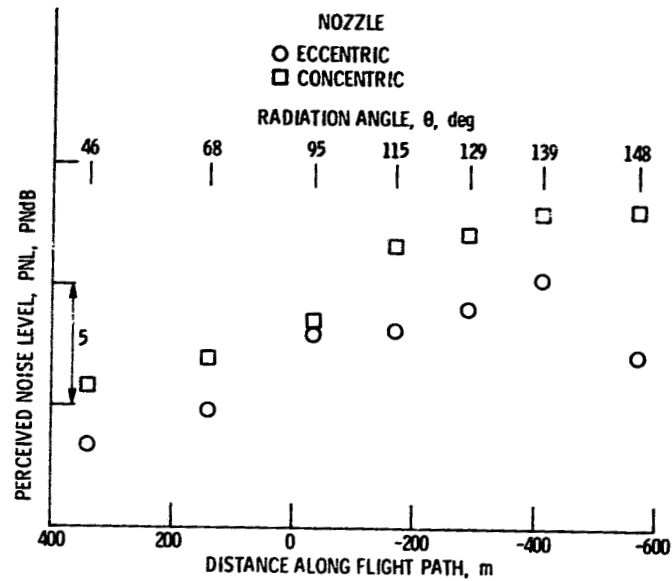
Figure 11. - Representative flyover PNL comparison between eccentric and concentric nozzles. Nominal values of: V_o, 229 m/s; V_i, 495 m/s; PR_o, 1.4; PR_i, 2.2; φ, 0°; flyover height, 338 m.

	PR_o	PR_i	V_o, m/s	V_i, m/s
○	1.4	1.8	232	601
□	1.4	1.4	229	338
◇	1.4	2.2	229	495

RADIATION ANGLE, θ, deg

46   68   95   115   129   139   148

-5

CHANGE IN PERCEIVED NOISE LEVEL, PNL_E - PNL_C, PNdB

0

5

(a) BOTH STREAMS SUBSONIC.

-6

-3

0

400   200   0   -200   -400   -600
DISTANCE ALONG FLIGHT PATH, m

(b) INNER STREAM SUPERSONIC, OUTER STREAM SUBSONIC.
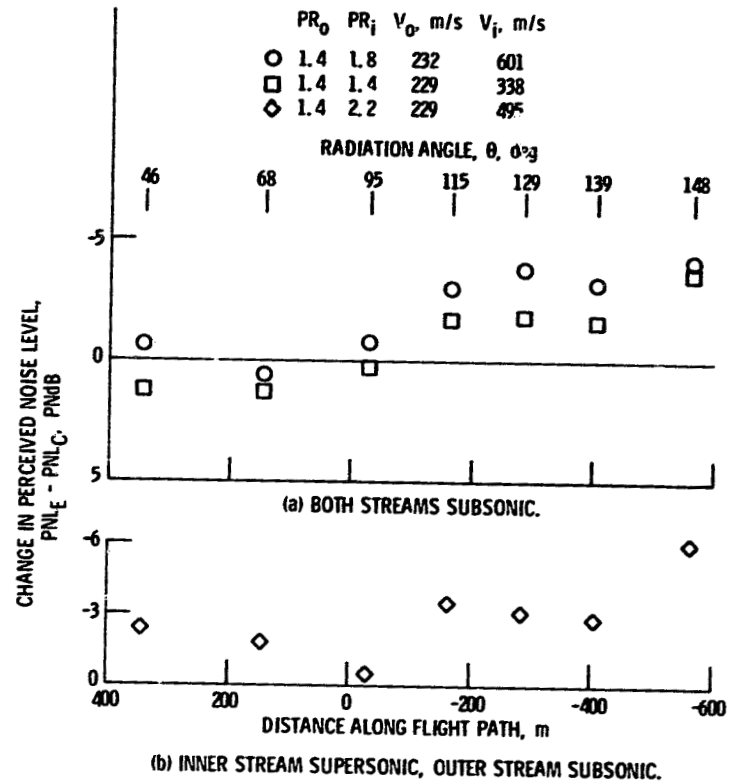
Figure 12. - Variation of PNL differences between concentric and eccentric nozzles as function of flyover distance.
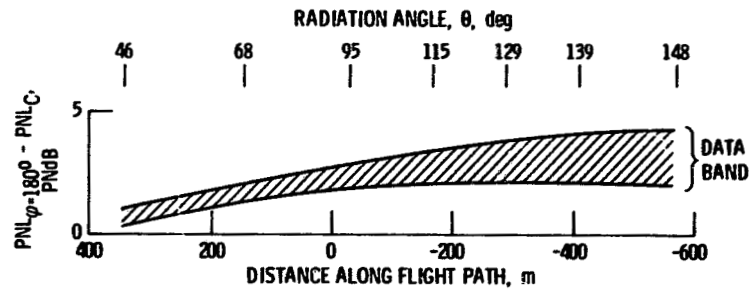
Figure 13. - Increase in PNL in plane of narrow annulus, $PNL_{\varphi=180^\circ}$ - PNLC, as function of flyover distance.
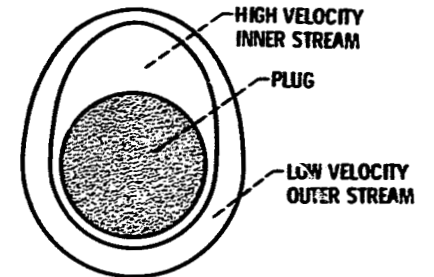

Figure 15. - Schematic of a possible conventional-bypass plug shaped-nozzle concept.

(a) PRESENT ECCENTRIC NOZZLE.

(b) PROPOSED ASYMMETRIC SHAPED NOZZLE.
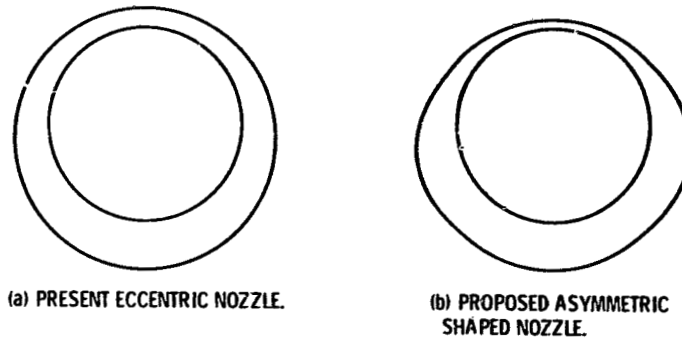
Figure 14. - Schematic annulus shaping for improved sideline noise suppression benefits.